ACS Medicinal Chemistry Letters
Cite This: ACS Med. Chem. Lett. XXXX, XXX, XXX−XXX
Letter
pubs.acs.org/acsmedchemlett

Mitochondrial Impairment by Cyanine-Based Small Molecules Induces Apoptosis in Cancer Cells

Sohan Patil,[†] Deepshikha Ghosh,[§] Mithun Radhakrishna,[∥] and Sudipta Basu*[,‡]

[†]Department of Chemistry, Indian Institute of Science Education and Research (IISER)-Pune, Dr. Homi Bhabha Road, Pashan, Pune, Maharashtra 411008, India

[‡]Discipline of Chemistry, [§]Discipline of Biological Engineering, and [∥]Discipline of Chemical Engineering of Indian Institute of Technology (IIT)-Gandhinagar, Palaj, Gandhinagar, Gujarat 382355, India

Supporting Information

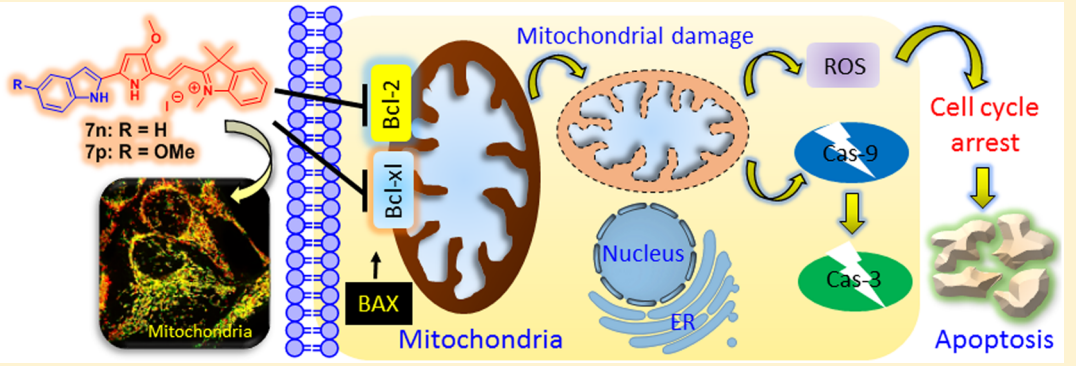

ABSTRACT: Mitochondrion, the powerhouse of the cells, has emerged as one of the unorthodox targets in anticancer therapy due to its involvement in several cellular functions. However, the development of small molecules for selective mitochondrial damage in cancer cells remained limited and less explored. To address this, in our work, we have synthesized a natural product inspired cyanine-based 3-methoxy pyrrole small molecule library by a concise strategy. This strategy involves Vilsmeier and Pd(0) catalyzed Suzuki cross-coupling reactions as key steps. The screening of the library members in HeLa cervical cancer cells revealed two new molecules that localized into subcellular mitochondria and damaged them. These small molecules perturbed antiapoptotic (Bcl-2/Bcl-xl) and pro-apoptotic (Bax) proteins to produce reactive oxygen species (ROS). Molecular docking studies showed that both molecules bind more tightly with the BH3 domain of Bcl-2 proteins compared to obatoclax (a pan-Bcl-2 inhibitor). These novel small molecules arrested the cell cycle in the G0/G1 phase, cleaved caspase-3/9, and finally prompted late apoptosis. This small molecule-mediated mitochondrial damage induced remarkably high cervical cancer cell death. These unique small molecules can be further explored as chemical biology tools and next-generation organelle-targeted anticancer therapy.

KEYWORDS: *Mitochondria, Suzuki cross-coupling, cell cycle arrest, apoptosis, cancer*

Mitochondrion (the powerhouse of the cells) is one of the most central organelles which controls ATP (energy currency) synthesis, retro-/anterograde signaling, biosynthesis, stress response, and storage of genomic materials.[1−5] Different stages of cancer development and progression involve alteration in mitochondrial functions.[6−9] Hence, targeting mitochondrial proteins and genomic materials has emerged as an unconventional strategy in cancer therapy.[10−13] Clinically approved small molecule anticancer drugs have been chemically tagged with cationic moieties (triphenylphosphonium ion and peptides) to detour them into mitochondria. This strategy improved drug efficacy, overcame drug resistance, and reduced off-target adverse effects.[14−18] Nevertheless, the development of novel small molecules to target mitochondrial functions in cancer cells is still in its infancy. In this direction, a few small molecules have been identified and synthesized to directly perturb mitochondrial translational machinery, ion channels, fission-fusion, and heat-shock proteins.[19−22] Hence, there is an urgent need to develop novel and easily synthesizable small molecules to impair mitochondria in cancer cells for next-generation anticancer therapy.[23]

To address this, we report a short and concise synthesis of cyanine-based 3-methoxy pyrrole derivatives. 3-Methoxy pyrrole is a privileged structure present in the Prodigiosin family of natural products with a broad range of anticancer activities.[24−29] We introduce a cyanine moiety due to its presence in MitoTracker Deep Red (mitochondria localizing dye) (Scheme 1a). Screening of these small library members in

Received: July 8, 2019
Accepted: December 10, 2019
Published: December 10, 2019

DOI: 10.1021/acsmedchemlett.9b00304
ACS Med. Chem. Lett. XXXX, XXX, XXX−XXX

Scheme 1. (a) Chemical Structures of 3-Methoxy-Pyrrole Based Biologically Active Natural Products, MitoTracker Deep Red, and Focused Library. (b) Synthetic Scheme of Cyanine-Based 3-Methoxy-Pyrrole Library. (c) Schematic Representation of Compounds 7n and 7p Impairing Mitochondria in Cancer Cells toward Apoptosis. (d) ORTEP Diagram of Compound 7d with 50% Thermal Ellipsoids

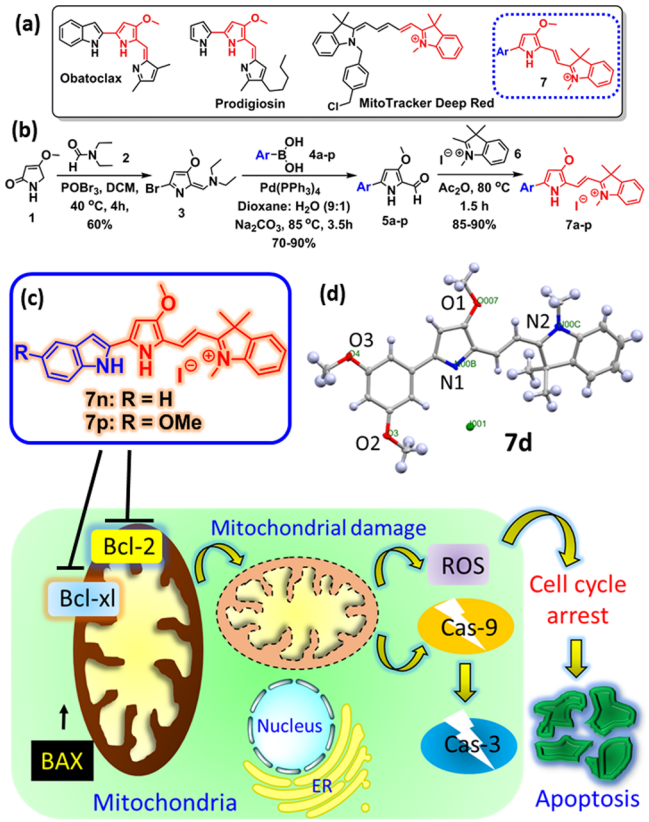

HeLa cervical cancer cells identified two highly potent new small molecules which localized into mitochondria and impaired them. These novel lead molecules inhibited antiapoptotic Bcl-2/Bcl-xl, activated pro-apoptotic Bax, and generated reactive oxygen species (ROS). These novel small molecule-mediated mitochondrial damages triggered cell cycle arrest in the G0/G1 phase and induced late apoptosis. This mitochondrial damage resulted in remarkable HeLa cervical cancer cell death at submicromolar concentration compared to clinically approved drugs (Scheme 1c).

The synthesis of cyanine-based 3-methoxy pyrrole is illustrated in Scheme 1b. We first reacted 4-methoxy-3-pyrroline-2-one (**1**) with *N*,*N*-diethyl formamide (**2**) in the presence of phosphorus oxybromide to obtain the 5-bromo-3-methoxy pyrrolidine derivative (**3**) (yield = 60%) through a modified Vilsmeier reaction. Compound **3** was then exposed to C−C bond formation by Suzuki cross-coupling reaction. We reacted compound **3** with aromatic boronic acids (**4a**−**p**) (Figure S1), in the presence of tetrakis(triphenylphosphine) palladium(0) as a catalyst to afford aromatic substituted 3-methoxy-pyrrole aldehydes (**5a**−**p**) in 70−90% yield (Figure S2). Finally, the aldehydes were condensed with 1,2,3,3-tetramethyl-3-H-indolium iodide (**6**) in the presence of acetic anhydride as a dehydrating agent to achieve focused library members. A library of 16 cyanine-based 3-methoxy-pyrroles (**7a**−**p**) was synthesized (Table 1, Figure S3). The chemical structures of all the intermediates and the final library members

Table 1. Compound Library (7a−p)

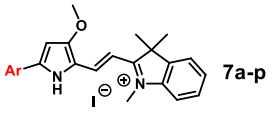

Compound	Ar	Compound	Ar
7a		7i	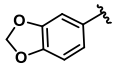
7b	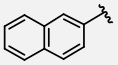	7j	
7c	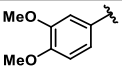	7k	
7d	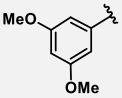	7l	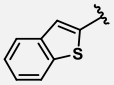
7e	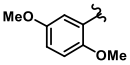	7m	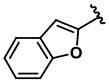
7f	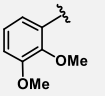	7n	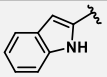
7g	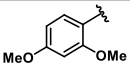	7o	
7h	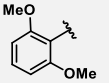	7p	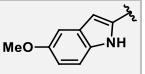

were confirmed by ^{1}H, ^{13}C NMR, and HR-MS spectroscopy (Figure S4−S102). Furthermore, we also confirmed the structure of one of the library members (**7d**) by X-ray crystallography (Scheme 1d, Table S1). Interestingly, all the library members were found to be red fluorescent in nature with a range of emission from λ_{max} = 556−593 nm (Figure S103, Table S2). This result was suitable for subcellular visualization.

We tested the library members for their cancer cell killing ability. We incubated HeLa cervical cancer cells with compounds **7a**−**7p** in a concentration-dependent manner for 24 h. Excitingly, the library members showed remarkable dose-dependent HeLa cell killing ability with IC_{50} values ranging from 4.47 to 0.92 μM (Figure 1, Table S3). We chose compounds **7n** and **7p** for further studies due to their best cell killing ability with IC_{50} = 0.97 and 0.92 μM, respectively. We also compared the efficacy of compounds **7n** and **7p** with clinically approved anticancer drugs (obatoclax, cisplatin, SN38, doxorubicin, and paclitaxel) in a dose-dependent manner for 24 h by MTT assay. To our delight, we found that cisplatin and SN38 showed negligible cell death even at 10 μM concentrations. However, obatoclax and paclitaxel showed moderate activity with cell viability of 70.35 ± 5.0% and 68.74 ± 3.2%, respectively (Figure S104). Only doxorubicin demonstrated comparable cancer cell killing with IC_{50} = 2.0 μM, that is as per our previous study.[30,31] We further evaluated the effect of **7n** and **7p** in noncancerous HEK293 human

DOI: 10.1021/acsmedchemlett.9b00304
ACS Med. Chem. Lett. XXXX, XXX, XXX−XXX

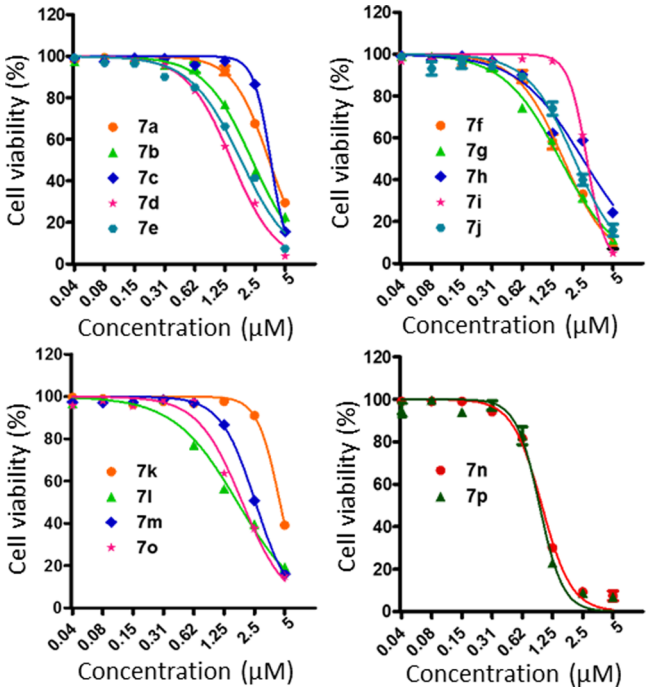

Figure 1. Dose-dependent cell viability assay of all the library members in HeLa cells at 24 h postincubation.

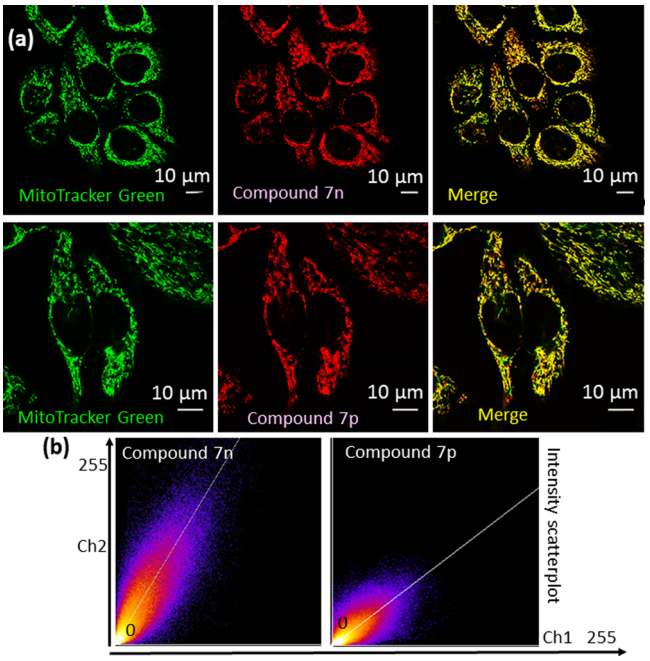

Figure 2. (a) Confocal laser scanning microscopy images of HeLa cells incubated with compounds **7n** and **7p** for 20 min. The mitochondria were stained with green fluorescent MitoTracker Green dye. The colocalization of compounds **7n** and **7p** was seen by merged yellow regions. (b) Intensity scatter plots of compounds **7n** and **7p** showing colocalization into mitochondria from confocal microscopy.

embryonic kidney cells for 24 h postincubation. We found that **7n** and **7p** showed much higher IC_{50} values of 2.56 and 2.61 μM with 24 and 25% of cell viability (at 5 μM), respectively, compared to HeLa cells (Figure S105).

We hypothesized that these novel cyanine-based 3-methoxypyrroles would induce mitochondrial impairment. To validate our hypothesis, we first observed the subcellular localization of compounds **7n** and **7p** into mitochondria by confocal laser scanning microscopy. HeLa cells were incubated with compounds **7n** and **7p** at 150 nM concentration for 20 min, followed by staining mitochondria by green fluorescent MitoTracker Green dye. The live HeLa cell imaging under confocal microscopy revealed that red fluorescent compounds **7n** and **7p** localized into green fluorescently tagged mitochondria to yield merged yellow signals (Figure 2a, Figure S106a). Intensity scatter plots of both the compounds also confirmed remarkable colocalization (Figure 2b). Further, z-stack maximum projection images obtained from confocal imaging (Figure S106b) also validated that compounds **7n** and **7p** homed into mitochondria of HeLa cells within 20 min.

When inside mitochondria, the lead compounds **7n** and **7p** should open up mitochondrial permeability transition pores (MPTPs), leading to the reduction in mitochondrial membrane potential ($\Delta\Psi m$) followed by rupture of the outer membrane.[32] We evaluated the opening of MPTPs by compounds **7n** and **7p** by Calcein AM assay.[33] To estimate MPTP formation, we treated HeLa cells with compounds **7n** and **7p** for 24 h followed by incubation with Calcein AM and $CoCl_2$. The live HeLa cells were visualized by confocal microscopy. The confocal images (Figure 3a, S107a) of nontreated control cells hardly showed any green fluorescent signal. On the other hand, compound **7n** and **7p** treated cells demonstrated a remarkable increase in green fluorescence intensity (3.6-fold and 3.9-fold, respectively, Figure S107b), consistent with our previous observation of MPTP formation.[34,23] These confocal images confirmed that compounds **7n** and **7p** induced mitochondrial damage by opening MPTPs in HeLa cells.

We further evaluated the morphological change as an indication of mitochondrial damage by **7n** and **7p**.[23] HeLa cells were treated with 500 nM of **7n** and **7p** for 3 h. The mitochondrial morphology was visualized by confocal imaging. The control cells were stained with MitoTracker Green. From the confocal imaging, we observed that **7n** and **7p** indeed damaged the mitochondria into smaller fragments (Figure S108a). In contrast, we observed elongated and filamentous mitochondrial morphology in the control cells. Further quantification from confocal microscopy also revealed that **7n** and **7p** induced the reduction in the average mitochondrial area by 3.4-fold and 2.6-fold, respectively, compared to control cells (Figure S108b). These confocal images confirmed that **7n** and **7p** damaged mitochondria.

The mitochondrial damage through MPTP formation was triggered by suppression of antiapoptotic Bcl-2/Bcl-xl proteins and activation of pro-apoptotic Bax.[35] Hence, we evaluated the expression of Bcl-2, Bcl-xl, and Bax by confocal microscopy. HeLa cells were treated with compounds **7n** and **7p** for 24 h followed by incubation with Bcl-2, Bcl-xl, and Bax primary antibodies. These primary antibodies were further recognized by Alexa Fluor 488 tagged (green-fluorescent) secondary antibody. The nuclei of the cells were counterstained by DAPI (blue). Fluorescence confocal microscopy showed high green fluorescence in control cells, confirming the presence of Bcl-2 and Bcl-xl (Figure 3b, c, Figure S109a, Figure S110a). However, treatment of compounds **7n** and **7p** showed a remarkable reduction in green fluorescence intensity into HeLa cells. This result validated the inhibition of antiapoptotic Bcl-2 and Bcl-xl. Further quantification from confocal images confirmed that compound **7n** reduced the green fluorescence

DOI: 10.1021/acsmedchemlett.9b00304
ACS Med. Chem. Lett. XXXX, XXX, XXX−XXX

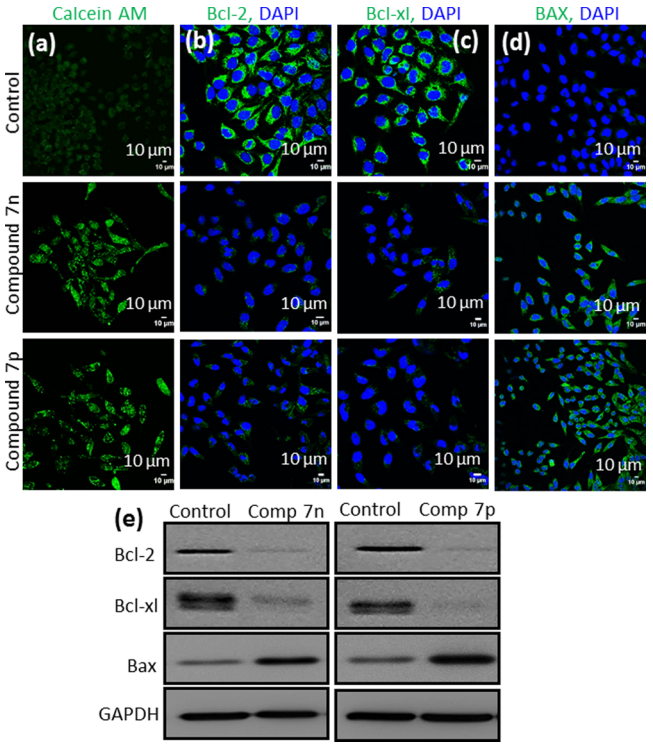

Figure 3. Confocal microscopy images of HeLa cells treated with compounds **7n** and **7p** for 24 h followed by (a) staining with Calcein AM to observe mitochondrial permeability transition pore opening (MPTPs). (b–d) Staining with Bcl-2, Bcl-xl, and Bax primary antibodies and green fluorescent Alexa Fluor 488-secondary antibody, respectively. Nuclei were stained with blue fluorescent DAPI dye. Scale bar = 10 μm. (e) Western blot analysis of Bcl-2, Bcl-xl, and Bax in HeLa cells after treatment with compounds **7n** and **7p** for 24 h.

intensity for Bcl-2 and Bcl-xl by 8.5-fold and 10.1-fold, respectively (Figure S109b, Figure S110b). Compound **7p** also reduced the green fluorescence intensity for Bcl-2 and Bcl-xl by 5.7-fold and 8.4-fold, respectively, compared to control cells (Figure S109b, Figure S110b). On the other hand, confocal images (Figure 3d, Figure S111a) and quantification (Figure S111b) showed that compounds **7n** and **7p** increased the expression of pro-apoptotic Bax proteins by 2.1-fold and 2.4-fold, respectively, compared to control cells.

We validated the inhibition of Bcl-2/Bcl-xl and activation of Bax by gel electrophoresis. HeLa cells were treated with compounds **7n** and **7p** for 24 h, and the cellular proteins were subjected to Western blot analysis. The Western blot images and quantification showed that compound **7n** reduced the expression of Bcl-2 and Bcl-xl by 6.4-fold and 4.0-fold, respectively (Figure 3e, Figure S112a,b). Compound **7p** treatment reduced the expressions of Bcl-2 and Bcl-xl by 9.3-fold and 5.6-fold, respectively (Figure 3e, Figure S112a,b). However, the expression of Bax was remarkably increased by compounds **7n** and **7p** by 3.6-fold and 4.1-fold, respectively (Figure 3e, Figure S112c). These confocal microscopy and Western blot studies confirmed that compounds **7n** and **7p** inhibited antiapoptotic Bcl-2/Bcl-xl and activated pro-apoptotic Bax proteins, which led to mitochondrial damage.

Compounds **7n** and **7p** are structurally similar to obatoclax, which binds with the BH3 domain of Bcl-2 proteins.[36] Hence, we carried out molecular docking studies using Auto Dock Vina in conjunction with MGL, ADT, and PMV software to quantify the binding affinity.[37,38] From these docking studies, the binding affinities of **7n** and **7p** in the BH3 domain of Bcl-2 were found to be −12 and −12.4 kcal/mol, respectively. These binding affinities were higher than the binding affinity of obatoclax (−6.5 kcal/mol) (Table S4). These docking studies confirmed that **7n** and **7p** binding with the BH3 domain of Bcl-2 was stronger than obatoclax leading to improved inhibition and cell killing.

This small molecule-mediated mitochondrial damage would lead to the generation of reactive oxygen species (ROS).[28] We evaluated ROS generation by 2′,7′-dichlorodihydrofluorescein (H_2DCFDA) assay.[39] HeLa cells were treated with compounds **7n** and **7p**, followed by incubation with H_2DCFDA. We then visualized the cells under a fluorescence microscope. The confocal images (Figure S113a) showed that control cells hardly generated any green fluorescent signals indicating negligible ROS generation. However, compound **7n** and **7p** treated cells showed a remarkable increase in green fluorescent signal intensity (16.1-fold and 22.4-fold, respectively) confirming the production of subcellular ROS (Figure S113b). This microscopy assay established that compounds **7n** and **7p** generated reactive oxygen species upon mitochondrial impairment.

Mitochondrial damage through inhibition of Bcl-2/Bcl-xl and ROS generation led to cell cycle arrest.[40] We treated HeLa cells with compounds **7n** and **7p** for 24 h and stained cellular DNA by propidium iodide (PI). We assessed the cells in different phases of the cell cycle by flow cytometry. The flow cytometry data revealed that 4.7%, 67.9%, 6.4%, and 16.8% of the cells were in the apoptotic, G0/G1, S, and G2-M phase after treatment with compound **7n**, respectively. In contrast, only 1.2%, 47.4%, 13.8%, and 33.9% of the cells were found in the apoptotic, G0/G1, S, and G2-M phase, respectively, for control cells (Figure 4a). Similarly, after treatment with compound **7p**, 3.5%, 63.9%, 13.5%, and 15.0% of the cells were found in the apoptotic, G0/G1, S and G2-M phase, respectively. This flow cytometry analysis exhibited that both compounds **7n** and **7p** induced cell cycle arrest in the G0/G1 phase after mitochondrial damage.

Mitochondrial damage and cell cycle arrest would trigger programmed cell death or apoptosis.[40,41] We quantified the induction of apoptosis by flow cytometry after treatment of HeLa cells with compounds **7n** and **7p** for 24 h. We further stained phosphatidylserine (at the outer membrane of apoptotic cells) and nuclear DNA (in necrotic cells) by Allophycocyanine (APC)-tagged Annexin V and 7-amino-actinomycin D (7-AAD), respectively. The cells were then sorted by flow cytometry, which demonstrated that both compounds **7n** and **7p** remarkably induced 99.5% and 98.7% cells into the late apoptotic stage, respectively (Figure 4b). The induction of late apoptosis was further validated by Western blot analysis. We evaluated the cleavage of initiator caspase-9 and executioner caspase-3 as apoptosis markers.[42,43] We incubated HeLa cells with compounds **7n** and **7p** for 24 h, and the whole-cell proteins were subjected to gel electrophoresis. The Western blot images explicitly showed that the expression of caspase-3 was reduced significantly to 3.5-fold and 3.7-fold by compounds **7n** and **7p**, respectively, compared to control cells (Figure 4c, Figure S114a). Similarly, compounds **7n** and **7p** also reduced the expression of caspase-9 to 1.9- and 2-fold, respectively (Figure 4c, Figure S114b). These flow cytometry and gel electrophoresis analyses confirmed that compounds **7n** and **7p** activated late apoptosis through cleavage of the caspase-3/9-based intrinsic pathway.

DOI: 10.1021/acsmedchemlett.9b00304
ACS Med. Chem. Lett. XXXX, XXX, XXX−XXX

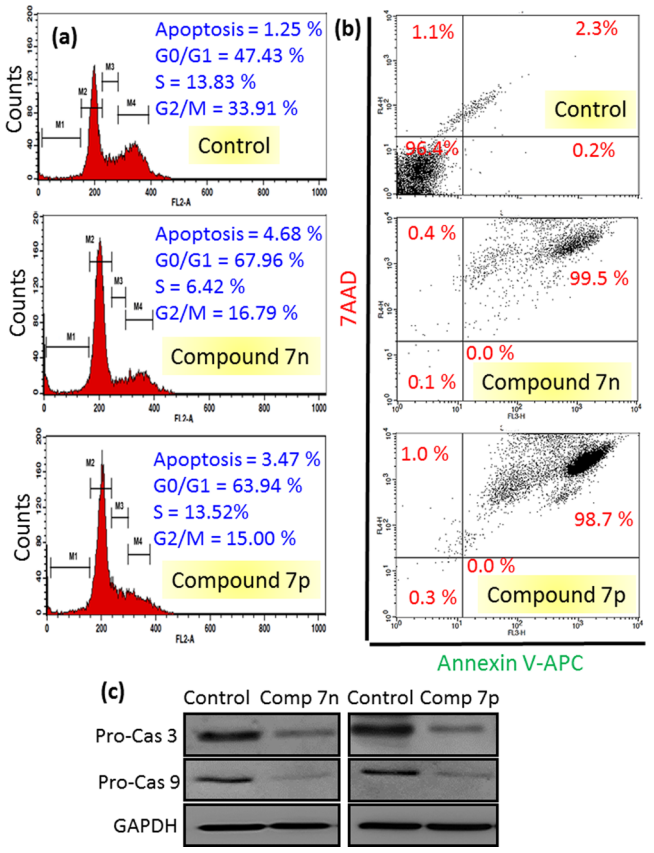

Figure 4. (a) Cell cycle analysis by staining the DNA in HeLa cells with PI at 24 h postincubation with compounds **7n** and **7p**. (b) Flow cytometry analysis of HeLa cells after treatment with compounds **7n** and **7p** for 24 h to observe apoptosis. (c) Western blot analysis to observe the expression of pro-caspase-3 and pro-caspase-9 in HeLa cells after treatment with compounds **7n** and **7p** for 24 h.

In conclusion, this report describes a short and straightforward synthesis of the natural product inspired cyanine based 3-methoxy pyrrole library. Two of the library members were found to be localized into mitochondria and impaired them. These novel small molecules inhibited anti-apoptotic Bcl-2/Bcl-xl and activated pro-apoptotic Bax proteins, followed by the production of reactive oxygen species in HeLa cervical cancer cells. These newly synthesized small molecules arrested the cell cycle in the G0/G1 phase. They cleaved caspase-3/9 to trigger apoptosis leading to improved cell death with IC_{50} = 0.9 μM. We anticipate that these unique small molecules can serve as chemical biology tools to understand mitochondrial functions in cancer cells. Furthermore, these novel small molecules can also open up new directions in organelle-targeted photodynamic anticancer therapy.

■ ASSOCIATED CONTENT

Supporting Information

The Supporting Information is available free of charge at https://pubs.acs.org/doi/10.1021/acsmedchemlett.9b00304.

Experimental details for chemical synthesis, cell culture, in vitro biological assays, spectroscopic characterization of the compounds, ^{1}H and ^{13}C NMR spectra, HR-MS spectra, absorption-emission spectra, MTT assay, confocal microscopy, quantification of proteins from Western blots, crystal data, photophysical data, and IC_{50} (PDF)

■ AUTHOR INFORMATION

Corresponding Author

*E-mail: sudipta.basu@iitgn.ac.in.

ORCID

Sohan Patil: 0000-0003-0940-9948

Mithun Radhakrishna: 0000-0001-7127-4744

Sudipta Basu: 0000-0002-0433-8899

Notes

The authors declare no competing financial interest.

■ ACKNOWLEDGMENTS

This project was financially supported by the Department of Biotechnology (BT/RLF/Re-entry/13/2011 and BT/PR14724/NNT/28/831/2015) and Department of Science and Technology, Govt. of India [SB/NM/NB-1083/2017 (G)]. S. Patil sincerely thanks CSIR-UGC for a fellowship. We sincerely thank Ravindra Raut of IISER-Pune for helping in X-ray crystallography analysis. We also thank Monal Desai and Akanksha Tripathi of the Writing Studio, IIT-Gandhinagar for helping in manuscript preparation.

■ REFERENCES

(1) Trifunovic, A.; Wredenberg, A.; Falkenberg, M.; Spelbrink, J. N.; Rovio, A. T.; Bruder, C. E.; Bohlooly, M.; Gidlöf, S.; Oldfors, A.; Wibom, R.; Törnell, J.; Jacob, H. T.; Larsson, N. Premature ageing in mice expressing defective mitochondrial DNA polymerase. *Nature* **2004**, *429*, 417−423.

(2) Smith, R. A. J.; Hartley, R. C.; Cochemé, H. M.; Murphy, M. P. Mitochondrial pharmacology. *Trends Pharmacol. Sci.* **2012**, *33*, 341−352.

(3) Ward, P. S.; Thompson, C. B. Metabolic reprogramming: a cancer hallmark even warburg did not anticipate. *Cancer Cell* **2012**, *21*, 297−308.

(4) Chandel, N. S. Mitochondria as signaling organelles. *BMC Biol.* **2014**, *12*, 34−40.

(5) Galluzzi, L.; Oliver, K.; Guido, K. Mitochondria: master regulators of danger signalling. *Nat. Rev. Mol. Cell Biol.* **2012**, *13*, 780−788.

(6) Calvo, S. E.; Mootha, V. K. The mitochondrial proteome and human disease. *Annu. Rev. Genomics Hum. Genet.* **2010**, *11*, 25−44.

(7) Nunnari, J.; Suomalainen, A. Mitochondria: in sickness and in health. *Cell* **2012**, *148*, 1145−1159.

(8) Gogvadze, V.; Orrenius, S.; Zhivotovsky, B. Mitochondria in cancer cells: what is so special about them? *Trends Cell Biol.* **2008**, *18*, 165−173.

(9) Boroughs, L. K.; DeBerardinis, R. J. Metabolic pathways promoting cancer cell survival and growth. *Nat. Cell Biol.* **2015**, *17*, 351−359.

(10) Fulda, S.; Galluzzi, L.; Kroemer, G. Targeting mitochondria for cancer therapy. *Nat. Rev. Drug Discovery* **2010**, *9*, 447−464.

(11) Weinberg, S. E.; Chandel, N. S. Targeting mitochondria metabolism for cancer therapy. *Nat. Chem. Biol.* **2015**, *11*, 9−15.

(12) Wallace, D. C. Mitochondria and cancer. *Nat. Rev. Cancer* **2012**, *12*, 685−698.

(13) Vyas, S.; Zaganjor, E.; Haigis, M. C. Mitochondria and cancer. *Cell* **2016**, *166*, 555−566.

(14) Marrache, S.; Pathak, R. K.; Dhar, S. Detouring of cisplatin to access mitochondrial genome for overcoming resistance. *Proc. Natl. Acad. Sci. U. S. A.* **2014**, *111*, 10444−10449.

(15) Jean, S. R.; Ahmed, M.; Lei, E. K.; Wisnovsky, S. P.; Kelley, S. O. Peptide-mediated delivery of chemical probes and therapeutics to mitochondria. *Acc. Chem. Res.* **2016**, *49*, 1893−1902.

DOI: 10.1021/acsmedchemlett.9b00304
ACS Med. Chem. Lett. XXXX, XXX, XXX−XXX

(16) Smith, R. A. J.; Porteous, C. M.; Gane, A. M.; Murphy, M. P. Delivery of bioactive molecules to mitochondria in vivo. *Proc. Natl. Acad. Sci. U. S. A.* **2003**, *100*, 5407−5412.
(17) Zielonka, J.; Joseph, J.; Sikora, A.; Hardy, M.; Ouari, O.; Vasquez-Vivar, J.; Cheng, G.; Kalyanaraman, B.; Lopez, M. Mitochondria-targeted triphenylphosphonium-based compounds: syntheses, mechanisms of action, and therapeutic and diagnostic applications. *Chem. Rev.* **2017**, *117*, 10043−10120.
(18) Wisnovsky, S.; Jean, S. R.; Liyanage, S.; Schimmer, A.; Kelley, S. O. Mitochondrial DNA repair and replication proteins revealed by targeted chemical probes. *Nat. Chem. Biol.* **2016**, *12*, 567−573.
(19) Škrtić, M.; Sriskanthadevan, S.; Jhas, B.; Gebbia, M.; Wang, X.; Wang, Z.; Hurren, R.; Jitkova, Y.; Gronda, M.; Maclean, N.; Lai, C. K.; Eberhard, Y.; Bartoszko, J.; Spagnuolo, P.; Rutledge, A. C.; Datti, A.; Ketela, T.; Moffat, J.; Robinson, B. H.; Cameron, J. H.; Wrana, J.; Eaves, C. J.; Minden, M. D.; Wang, J. C.; Dick, J. E.; Humphries, K.; Nislow, C.; Giaever, G.; Schimmer, A. D. Inhibition of mitochondrial translation as a therapeutic strategy for human acute myeloid leukemia. *Cancer Cell* **2011**, *20*, 674−688.
(20) Wang, D.; Wang, J.; Bonamy, G. M. C.; Meeusen, S.; Brusch, R. G.; Turk, C.; Yang, P.; Schultz, P. G. A small molecule promotes mitochondrial fusion in mammalian cells. *Angew. Chem., Int. Ed.* **2012**, *51*, 9302−9305.
(21) Leanza, L.; Romio, M.; Becker, A. K.; Azzolini, M.; Trentin, L.; Managò, A.; Venturini, E.; Zaccagnino, A.; Mattarei, A.; Carraretto, L.; Urbani, A.; Kadow, S.; Biasutto, L.; Martini, V.; Severin, F.; Peruzzo, R.; Trimarco, V.; Egberts, J. H.; Hauser, C.; Visentin, A.; Semenzato, G.; Kalthoff, H.; Zoratti, M.; Gulbins, E.; Paradisi, C.; Szabo, I. Direct pharmacological targeting of a mitochondrial ion channel selectively kills tumor cells in vivo. *Cancer Cell* **2017**, *31*, 516−531.
(22) Park, S.; Baek, K.; Shin, I.; Shin, I. Subcellular Hsp70 inhibitors promote cancer cell death via different mechanisms. *Cell Chem. Biol.* **2018**, *25*, 1242−1254.
(23) Patil, S.; Kuman, M. M.; Palvai, S.; Sengupta, P.; Basu, S. Impairing powerhouse in colon cancer cells by hydrazide−hydrazone-based small molecule. *ACS Omega* **2018**, *3*, 1470−1481.
(24) Fürstner, A. Chemistry and biology of roseophilin and the prodigiosin alkaloids: a survey of the last 2500 years. *Angew. Chem., Int. Ed.* **2003**, *42*, 3582−3603.
(25) Sessler, J. L.; Eller, L. R.; Cho, W.; Nicolaou, S.; Aguilar, A.; Lee, J. T.; Lynch, V. M.; Magda, D. J. Synthesis, anion-binding properties, and in vitro anticancer activity of prodigiosin analogues. *Angew. Chem.* **2005**, *117*, 6143−6146.
(26) Montaner, B.; Pérez-Tomás, R. The prodigiosins: a new family of anticancer drugs. *Curr. Cancer Drug Targets* **2003**, *3*, 57−65.
(27) Montaner, B.; Navarro, S.; Pique, M.; Vilaseca, M.; Martinell, M.; Giralt, E.; Gil, J.; Perez-Tomas, R. Prodigiosin from the supernatant of Serratia marcescens induces apoptosis in haematopoietic cancer cell lines. *Br. J. Pharmacol.* **2000**, *131*, 585−593.
(28) Schimmer, A. D.; O'Brien, S.; Kantarjian, H.; Brandwein, J.; Cheson, B. D.; Minden, M. D.; Yee, K.; Ravandi, F.; Giles, F.; Schuh, A.; Gupta, V.; Andreeff, M.; Koller, C.; Chang, H.; Kamel-Reid, S.; Berger, M.; Viallet, J.; Borthakur, G. A Phase I Study of the Pan Bcl-2 Family Inhibitor Obatoclax Mesylate in Patients with Advanced Hematologic Malignancies. *Clin. Cancer Res.* **2008**, *14*, 8295−8301.
(29) O'Brien, S. M.; Claxton, D. F.; Crump, M.; Faderl, S.; Kipps, T.; Keating, M. J.; Viallet, J.; Cheson, B. D. Phase I Study of Obatoclax Mesylate (GX15−070), a Small Molecule Pan-Bcl-2 Family Antagonist, in Patients with Advanced Chronic Lymphocytic Leukemia. *Blood* **2009**, *113*, 299−305.
(30) Mallick, A.; More, P.; Ghosh, S.; Chippalkatti, R.; Chopade, B. A.; Lahiri, M.; Basu, S. Dual drug conjugated nanoparticle for simultaneous targeting of mitochondria and nucleus in cancer cells. *ACS Appl. Mater. Interfaces* **2015**, *7*, 7584−7598.
(31) Palvai, S.; More, P.; Mapara, N.; Basu, S. Chimeric Nanoparticle: A Platform for Simultaneous Targeting of Phosphatidylinositol-3-Kinase Signaling and Damaging DNA in Cancer Cells. *ACS Appl. Mater. Interfaces* **2015**, *7*, 18327−18335.
(32) Tait, S. W. G.; Green, D. R. In vivo and in vitro determination of cell death markers in neurons. *Nat. Rev. Mol. Cell Biol.* **2010**, *11*, 621−632.
(33) Petronilli, V.; Miotto, G.; Canton, M.; Brini, M.; Colonna, R.; Bernardi, P.; Di Lisa, F. Transient and long-lasting openings of the mitochondrial permeability transition pore can be monitored directly in intact cells by changes in mitochondrial calcein fluorescence. *Biophys. J.* **1999**, *76*, 725−734.
(34) Mallick, A.; More, P.; Syed, M. M. K.; Basu, S. Nanoparticle-Mediated Mitochondrial Damage Induces Apoptosis in Cancer. *ACS Appl. Mater. Interfaces* **2016**, *8*, 13218−13231.
(35) Chipuk, J. E.; Green, D. R. How do BCL-2 proteins induce mitochondrial outer membrane permeabilization? *Trends Cell Biol.* **2008**, *18*, 157−164.
(36) Nguyen, M.; Marcellus, R. C.; Roulston, A.; Watson, M.; Serfass, L.; Murthy Madiraju, S. R.; Goulet, D.; Viallet, J.; Bélec, L.; Billot, X.; Acoca, S.; Purisima, E.; Wiegmans, A.; Cluse, L.; Johnstone, R. W.; Beauparlant, P.; Shore, G. C. Small Molecule Obatoclax (GX15−070) Antagonizes MCL-1 and Overcomes MCL-1-Mediated Resistance to Apoptosis. *Proc. Natl. Acad. Sci. U. S. A.* **2007**, *104*, 19512−19517.
(37) Maity, S.; Mukherjee, K.; Banerjee, A.; Mukherjee, S.; Dasgupta, D.; Gupta, S. Inhibition of Porcine Pancreatic Amylase Activity by Sulfamethoxazole: Structural and Functional Aspect. *Protein J.* **2016**, *35*, 237−246.
(38) Helgren, T. R.; Hagen, T. J. Demonstration of AutoDock as an Educational Tool for Drug Discovery. *J. Chem. Educ.* **2017**, *94*, 345−349.
(39) Wu, D.; Yotnda, P. Production and detection of reactive oxygen species (ROS) in cancers. *J. Visualized Exp.* **2011**, No. e3357.
(40) Koczor, C. A.; Shokolenko, I. N.; Boyd, A. K.; Balk, S. P.; Wilson, G. L.; LeDoux, S. P. Mitochondrial DNA damage initiates a cell cycle arrest by a Chk2-associated mechanism in mammalian cells. *J. Biol. Chem.* **2009**, *284*, 36191−36201.
(41) Czabotar, P. E.; Lessene, G.; Strasser, A.; Adams, J. M. Control of apoptosis by the BCL-2 protein family: implications for physiology and therapy. *Nat. Rev. Mol. Cell Biol.* **2014**, *15*, 49−63.
(42) Mariño, G.; Niso-Santano, M.; Baehrecke, E. H.; Kroemer, G. Self-consumption: the interplay of autophagy and apoptosis. *Nat. Rev. Mol. Cell Biol.* **2014**, *15*, 81−94.
(43) Li, P.; Nijhawan, D.; Budihardjo, I.; Srinivasula, S. M.; Ahmad, M.; Alnemri, E. S. X.; Wang, X. Cytochrome c and dATP-dependent formation of Apaf-1/caspase-9 complex initiates an apoptotic protease cascade. *Cell* **1997**, *91*, 479−489.

DOI: 10.1021/acsmedchemlett.9b00304
ACS Med. Chem. Lett. XXXX, XXX, XXX−XXX